07

AlGaAs subcells for hybrid A^3B^5//Si solar cells

© S.A. Mintairov, V.M. Emelyanov, N.A. Kalyuzhnyy, M.V. Nakhimovich, R.A. Salii, M.Z. Shvarts

Ioffe Institute, St. Petersburg, Russia
E-mail: mintairov@scell.ioffe.ru

Received August 26, 2025
Revised October 7, 2025
Accepted October 7, 2025

The values of diffusion lengths of minority charge carriers in $Al_xGa_{1-x}As$ (AlGaAs) layers with aluminum concentrations x from 0 to 0.2 were determined. For this the spectra of quantum yield for single-junction solar cells with photoactive layers based on AlGaAs have been approximated. The calculations of the external quantum efficiency spectra for GaInP, AlGaAs and Si subcells of hybrid GaInP/AlGaAs//Si solar cells (SC) for space applications are performed. It is shown that GaInP/AlGaAs//Si SCs provide an efficiency of 33.5 % (1 sun, AM0) with complete carriers collection from the base layer of the AlGaAs subcell and an aluminum concentration of $x = 0.1$, 33 % (1 sun, AM0) when using a gradient composition in the base layer and an average aluminum concentration of $x = 0.08$ and 32.8 % (1 sun, AM0) when using a constant aluminum concentration of $x = 0.08$.

Keywords: hybrid solar cells, subcell, MOVPE, efficiency, quantum efficiency, mathematical modeling.

DOI: 10.61011/TPL.2026.02.63038.20481

More than 6,000 satellites are currently orbiting the Earth, and more than half of them are used for various civilian purposes [1]: communications (Internet, cellular service, radio, television); global positioning (location services and navigation); Earth observation, sensing, and monitoring (weather tracking, disaster forecasting). The energy generation system is one of the most important components of spacecraft located both in near-Earth orbit and far from it.

The intensity of solar radiation in the Earth's outer atmosphere with the AM0 spectral distribution is $1367\,W/m^2$. Typical solar cells (SCs), which are the only source of energy for spacecraft, are heterostructure devices consisting of several different materials deposited epitaxially onto a substrate. The materials used most often in photovoltaic technologies for space applications are silicon and semiconductors found in multi-junction (MJ) solar cells: Ge; A^3B^5 semiconductors, such as GaAs and InP; and A^3B^5 solid solutions (InGaP, InGaAs, InGaNAs, AlInGaP, and AlInGaAs) [2].

Specifically, InGaP/InGaAs/Ge and AlInGaP/AlInGaAs/InGaAs/Ge MJ SCs produced by Azur Space, Spectrolab, SolAero, and CESI for various space missions are the current standard in aerospace engineering, since they provide better performance characteristics than other photovoltaic systems [2]. For example, commercially available AlInGaP/AlInGaAs/InGaAs/Ge MJ SCs produced by Azur Space have a conversion efficiency of up to 32 % (1 sun, AM0) at the start of their service life and 28.7 % (1 sun, AM0) at the end of service life (i. e., after irradiation with electrons with an energy of 1 MeV and a dose of $10^{15}\,cm^{-2}$), which is currently the best result for space SCs. Despite all this, MJ SCs have a number of disadvantages, such as rigidity, thickness (from ~ 80 to $\sim 200\,\mu m$), and high specific weight: the specific power of GaInP/Ga(In)As/Ge three-junction SCs is $\sim 0.4{-}0.8$ W/g [3,4], although the use of inverted cells may help raise the power up to 3.8 W/g for InGaP/GaAs/InGaAs SCs [5]. However, it is very hard to produce inverted MJ SCs, and such SCs are thus extremely expensive [6].

Current research activities in the field of innovative photovoltaic technologies for future space missions are focused not only on increasing the efficiency of SCs (due to higher power requirements), but also on improving their weight and size parameters. One possible solution to these problems is bonding of SCs based on A^3B^5 semiconductors and silicon SCs, since silicon is more lightweight than other materials applicable as a substrate for MJ solar cells. Since the thickness of an epitaxial structure ($5{-}7\,\mu m$) and metallic contacts ($2{-}3\,\mu m$) is much smaller than the thickness of a substrate ($80{-}200\,\mu m$), the weight of the latter is what determines the specific power of an MJ SC. The density of germanium ($5.323\,g/cm^2$) and gallium arsenide ($5.318\,g/cm^2$), which are used as substrates for MJ SCs, is more than 2 times higher than the density of silicon ($2.33\,g/cm^2$). This suggests that the specific power density of A_3B_5//Si hybrid solar cells (HSCs) may increase by a factor of more than 2 relative to that for MJ SCs grown on Ge and GaAs substrates. Efficient bonding of GaInP/GaAs and GaInP/GaInAsP two-junction tandem cells with single-junction Si SCs has recently been demonstrated in [7,8].

Our previous study [9] was focused on calculating the external quantum yield spectra for GaInP, Ga(In)As, and Si subcells of GaInP/Ga(In)As//Si space-grade HSCs. It was demonstrated that the substitution of middle and bottom subcells in a GaInP/Ga(In)As/Ge structure with GaAs and Si, respectively, helps increase the efficiency from 29.4 to 30.8 % (1 sun, AM0) while also improving the energy-

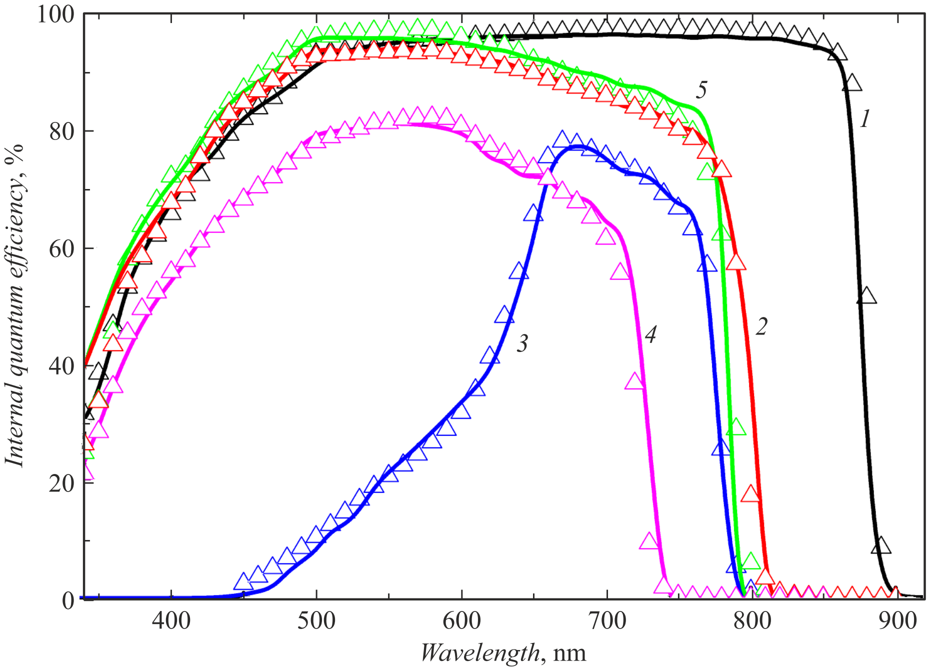

Figure 1. Measured (symbols) and calculated (curves) spectra of internal quantum efficiency for SCs based on GaAs (*1*), $Al_{0.11}Ga_{0.89}As$ (*2*), $Al_{0.14}Ga_{0.86}As$ with a GaInP optical filter 350 nm in thickness (*3*), $Al_{0.2}Ga_{0.8}As$ (*4*), and a gradient base layer composition changing from $Al_{0.15}Ga_{0.85}As$ to $Al_{0.11}Ga_{0.89}As$ (*5*).

mass parameters and extending the active service life of space solar batteries.

The present study details further optimization of the GaInP/GaAs//Si HSC structure via the introduction of aluminum atoms into the photoactive layers of the middle (GaAs) subcell. An increase in band gap width of HSC subcells will lead to an increase in voltage generated by them, which, in turn, should enhance the HSC efficiency. However, the introduction of aluminum into gallium arsenide is known to induce a reduction in diffusion lengths of minority carriers, which may have a negative effect on the operation of the AlGaAs subcell.

In order to determine the diffusion lengths in AlGaAs layers, we grew SC structures based on GaAs, $Al_{0.11}Ga_{0.89}As$, $Al_{0.14}Ga_{0.86}As$ with a GaInP optical filter 350 nm in thickness, $Al_{0.2}Ga_{0.8}As$, and a gradient base layer composition changing from $Al_{0.15}Ga_{0.85}As$ to $Al_{0.11}Ga_{0.89}As$. The studied SC structures were grown by metalorganic vapor-phase epitaxy on a p^+-GaAs (100) substrate and included the following sequentially deposited layers: p-$Al_{0.3}Ga_{0.7}As$ back potential barrier 100 nm in thickness, p-$Al_xGa_{1-x}As$ base 3000 nm in thickness, n-$Al_xGa_{1-x}As$ emitter 100 nm in thickness, and n-$Al_{0.9}Ga_{0.1}As$ wide-band window 35 nm in thickness. The measured spectral characteristics of SCs fabricated from these structures are presented in Fig. 1 (symbols). Mathematical modeling of the spectral characteristics of single-junction $Al_xGa_{1-x}As$ SCs (curves in Fig. 1) was performed in accordance with the procedure outlined in [10] and allowed us to determine the diffusion lengths of minority carriers in the photoactive layers of AlGaAs (Fig. 2).

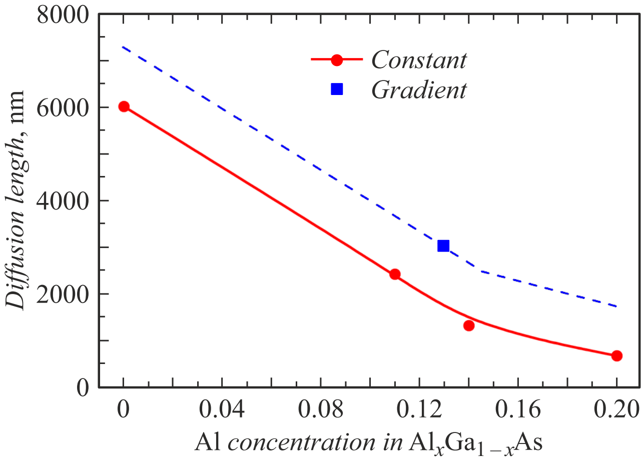

Figure 2. Dependences of the electron diffusion length in the AlGaAs base on the solid solution composition for constant (circles) and gradient (square) compositions. The dashed line represents the diffusion length approximation.

It is evident from Fig. 2 that an increase in aluminum concentration in the photoactive SC layers leads to a significant reduction in diffusion length in the base layer, where the bulk of photogenerated current (PGC) is collected. The introduction of a gradient base layer composition, which produces an electric pulling field for photogenerated carriers, helps mitigate this reduction to a certain extent (Fig. 2).

The diffusion length data were used to calculate the service and structural parameters of GaInP/AlGaAs//Si HSCs in three cases: complete collection of photogenerated carriers (the diffusion length in the base is much greater than its thickness), a gradient composition of the base layer (diffusion lengths represented by the dashed line in Fig. 2 were used), and a constant composition of the base layer in AlGaAs subcells (diffusion lengths represented by the solid line in Fig. 2 were used). PGCs were calculated using the method detailed in [10] by varying the thicknesses of photoactive layers of the top (GaInP) and middle (AlGaAs) subcells of GaInP/AlGaAs//Si HSCs until the PGCs of these subcells became equal. The open-circuit voltage and efficiency of HSCs were calculated in accordance with the procedure outlined in [9]. A GaInP/Ga(In)As/Ge SC with an efficiency of 29.4 % (1 sun, AM0) served as the reference.

The calculation results are shown in Fig. 3. The open-circuit voltage of GaInP/GaAs//Si HSCs is 3.24 V and increases with increasing aluminum concentration in the middle subcell (Fig. 3, *b*), and the calculated efficiency is 31.9 % (Fig. 3, *e*). Complete PGC matching at the level of 15.1 mA/cm^2 (Fig. 3, *a*) in GaInP/GaAs//Si HSCs is achieved with a thickness of photoactive layers of the top subcell of 340 nm (Fig. 3, *c*) and a thickness of photoactive layers of the middle subcell of 770 nm (Fig. 3, *d*). These thicknesses are significantly smaller than the corresponding thicknesses of the reference GaInP/Ga(In)As/Ge SC (dashed lines in Fig. 3).

The addition of aluminum to the photoactive layers of the middle subcell results in a shift of its absorption edge toward shorter wavelengths. This necessitates an increase in thickness of the base layer, which is needed to ensure absorption of the same number of photons (Fig. 3, *d*) and raises the requirements as to the electron diffusion length in the base layer of the $Al_xGa_{1-x}As$ subcell. This does not affect the collection of photogenerated carriers from the base layer (Fig. 3, *a*) at concentrations up to $x = 0.06$, but the PGC calculated with account for the previously determined diffusion lengths starts decreasing at higher x values (Fig. 3, *a*). Complete PGC matching in GaInP/$Al_xGa_{1-x}As$//Si HSCs is infeasible at $x > 0.1$, since too many photons enter the bottom (silicon) subcell, and the PGC starts decreasing even with complete collection from the base layer of the $Al_xGa_{1-x}As$ subcell (Fig. 3, *a*). The thickness of photoactive layers of the $Al_xGa_{1-x}As$ subcell then becomes equal to 5000 nm (Fig. 3, *d*), which is needed for complete absorption of all photons with energy greater than the band gap of $Al_xGa_{1-x}As$, and the thickness of photoactive layers of the GaInP subcell starts decreasing (Fig. 3, *c*) to let a certain fraction of photons pass into the $Al_xGa_{1-x}As$ subcell and increase its PGC.

The calculated data revealed (Fig. 3, *e*) that GaInP/$Al_xGa_{1-x}As$//Si HSCs provide an efficiency of 33.5 % (1 sun, AM0) with complete carrier collection and aluminum concentration $x = 0.1$; 33 % (1 sun, AM0) with a gradient composition and average aluminum concentration $x = 0.08$; and 32.8 % (1 sun, AM0) with a constant aluminum concentration $x = 0.08$.

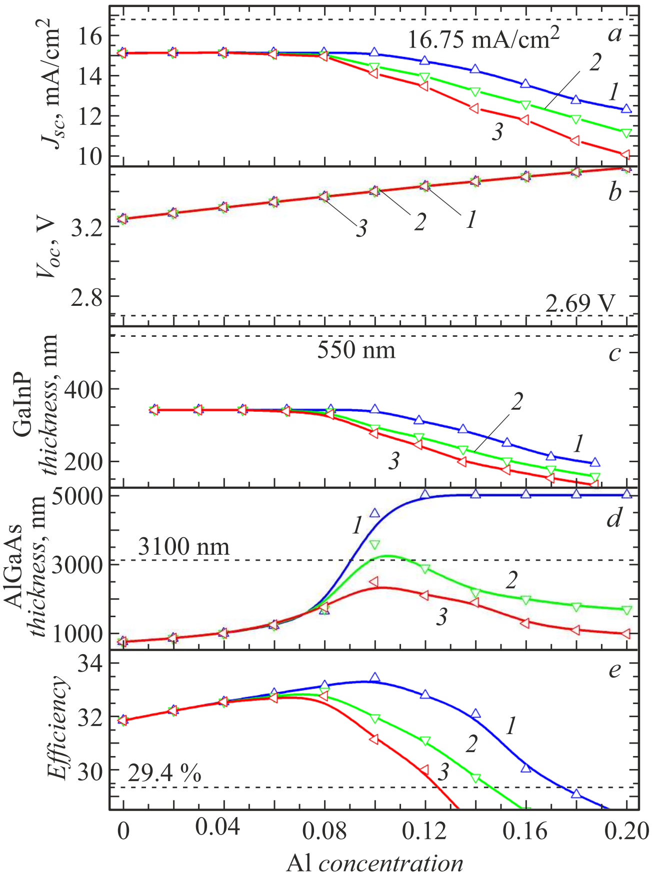

Figure 3. Dependences of short-circuit current (*a*), open-circuit voltage (*b*), thickness of photoactive layers of the GaInP subcell (*c*), thickness of photoactive layers of the AlGaAs subcell (*d*), and efficiency (*e*) of GaInP/AlGaAs//Si HSCs matched in PGC for complete collection of photogenerated carriers from the AlGaAs base layer (*1*), their collection according to diffusion lengths with a gradient base composition (*2*), and their collection according to diffusion lengths with a constant base composition (*3*). Dashed lines indicate the characteristics of the reference GaInP/Ga(In)As/Ge SC.

Conflict of interest

The authors declare that they have no conflict of interest.

References

[1] L. Greco, *UCS Satellite Database* [Electronic source]. https://www.ucsusa.org/resources/satellite-database

[2] R. Verduci, V. Romano, G. Brunetti, N.Y. Nia, A. Di Carlo, G. D'Angelo, C. Ciminell, Adv. Energy Mater., **12**, 2200125 (2022). DOI: 10.1002/aenm.202200125

[3] M. Kaltenbrunner, G. Adam, E.D. Głowacki, M. Drack, R. Schwödiauer, L. Leonat, D.H. Apaydin, H. Groiss, M.C. Scharber, M.S. White, N.S. Sariciftci, S. Bauer, Nat. Mater., **14**, 1032 (2015). DOI: 10.1038/nmat4388

[4] F. Lang, M. Jošt, K. Frohna, E. Köhnen, A. Al-Ashouri, A.R. Bowman, T. Bertram, A.B. Morales-Vilches, D. Koushik, E.M. Tennyson, K. Galkowski, G. Landi, M. Creatore, B. Stannowski, C.A. Kaufmann, J. Bundesmann, J. Rappich, B. Rech, A. Denker, S. Albrecht, H.C. Neitzert, N.H. Nickel, S.D. Stranks, Joule, **4**, 1054 (2020). DOI: 10.1016/j.joule.2020.03.006

[5] D. Cardwell, A. Kirk, C. Stender, A. Wibowo, F. Tuminello, M. Drees, R. Chan, M. Osowski, N. Pan, in *2017 IEEE 44th Photovoltaic Specialists Conf.* (PVSC) (IEEE, 2017), p. 3511. DOI: 10.1109/PVSC.2017.8366552

[6] J. Li, A. Aierken, Y. Liu, Y. Zhuang, X. Yang, J.H. Mo, R.K. Fan, Q.Y. Chen, S.Y. Zhang, Y.M. Huang, Q. Zhang, Front. Phys., **8**, 631925 (2021). DOI: 10.3389/fphy.2020.631925

[7] P. Schygulla, R. Müller, D. Lackner, O. Höhn, H. Hauser, B. Bläsi, F. Predan, J. Benick, M. Hermle, S. Glunz, F. Dimroth, Prog. Photovolt.: Res. Appl., **30**, 869 (2022). DOI: 0.1002/pip.3503

[8] P. Schygulla, R. Müller, O. Höhn, M. Schachtner, D. Chojniak, A. Cordaro, S. Tabernig, B. Bläsi, A. Polman, G. Siefer, D. Lackner, F. Dimroth, Prog. Photovolt.: Res. Appl., **33** (1), 100 (2025). DOI: 10.1002/pip.3769

[9] S.A. Mintairov, V.M. Emelyanov, N.A. Kalyuzhnyy, M.V. Nakhimovich, V.V. Oleynik, R.A. Salii, A.F. Skachkov, L.N. Skachkova, M.Z. Shvarts, Tech. Phys. Lett., **51** (7), 37 (2025). DOI: 10.61011/TPL.2025.07.61428.20295.

[10] S.A. Mintairov, V.M. Andreev, V.M. Emelyanov, N.A. Kalyuzhnyy, N.K. Timoshina, M.Z. Shvarts, V.M. Lantratov, Semiconductors, **44** (8), 1084 (2010). DOI: 10.1134/S1063782610080233.

Translated by D.Safin